Peer-reviewed version available at Materials 2019, 12, 4137; doi:10.3390/ma12244137

Article

Simple Calibration Method for Confocal Microscopy Used in Micro-Additive Manufacturing Processes

Alberto Mínguez Martínez [1,2,*] and Jesús de Vicente y Oliva [1,2,*]

[1] Laboratorio de Metrología y Metrotecnia, Escuela Técnica Superior de Ingenieros Industriales, Universidad Politécnica de Madrid; c./ José Gutiérrez Abascal, 2, 28006 Madrid, Spain
[2] Centro Láser, Universidad Politécnica de Madrid, Campus Sur, Edificio "La Arboleda"; c./ Alan Turing, 1, 28031 Madrid, Spain
* Correspondence: a.minguezm@upm.es (A.M.M.); jvo@etsii.upm.es (J.d.V.O.)

Abstract: Additive manufacturing (AM) is a promising new technology that is having a very fast growth from home workshops to high-tech cutting-edge factories. As any manufacturing technique, adequate metrology services are needed to assure the quality of items manufactured by AM. One of the most widely used instruments to measure the characteristics of surfaces manufactured with AM is the confocal microscope. In this paper, authors present a whole calibration procedure for confocal microscopes designed to be implemented preferably in workshops or industrial environments rather than in research and development departments. Because of that, it is as simple as possible. The procedure is designed without forgetting any of the key aspects that need to be taken into account and based on classical reference material standards. These standards can be easily found in industrial dimensional laboratories and easily calibrated in accredited calibration laboratories.

Keywords: additive manufacturing; confocal microscopy; measurement; calibration; traceability; uncertainty; quality assessment

---

1. Introduction

Additive manufacturing (AM) is a modern technology, developed in the mid 1980's, based on the creation of entire objects through the gradual accumulation of material layer by layer [1, 2, 3, 4, 5]. It has been the most important advance in manufacturing technologies in the last 30 years. This technology has different names, such as "Rapid Prototyping", "Solid Free-form Fabrication" or "Three-Dimensional Printing" [6]. As it is known, this technology starts from a Computer Aided Design (CAD) model, what enables to design three-dimensional physical entity models, and shapes them layer by layer, depositing each layer over the previous one [3]. This is achieved by using a computer program designed for creation of two-dimensional cross sections. Nowadays, AM is used mainly in aerospace and automotive industries as well as in medical applications [7, 8]. This kind of technology allows the design and manufacturing of infinite types of geometries, without the constrains usually found when subtractive techniques are used [9].

There are many AM processes apart from 3D printing: selective laser melting, selective laser sintering, stereolithography, fused deposition modeling, electron beam melting and laminated object processes. [4, 10, 11]

Despite the multiple benefits and options of additive manufacturing, it is important to note that this technology is currently being studied and it is still at an early stage of development. It seems that it will be a key manufacturing option in the near future [9].

According to several authors, there are many technologies at their first stages of development and their future is still unknown. There are many fields that can be studied, standing out the following [4, 7]:

- Materials.

- Design for AM.
- Micron-scale systems.
- Biomanufacturing.
- Modeling, sensing, control and process innovation.
- Characterization and certification.
- Integrated systems for Niche applications.

In the literature, the importance of two key parameters for AM processes is highlighted: dimensional accuracy and surface quality [8, 12]. On one hand, it is necessary to ensure dimensional accuracy and measurement traceability with a reasonable level of confidence so that manufacturers should be able to ensure the conformity with product specifications. On the other hand, it is necessary to have control over surface quality. For a correct deposition of each layer, it is necessary to have a controlled roughness value. Because of this kind of processes, AM manufactured parts usually have high values of this characteristic [9].

Since every manufacturing processes have a dimensional tolerance scheme, AM processes also need to go through metrological control. Traditional subtractive machines are verified using reference standards with suitable traceability [9]. We can define traceability as the property of a measurement result by which it can be related to a reference through an uninterrupted and documented chain of calibrations, each of which contributes to measurement uncertainty [13]. There are many traditional techniques in Dimensional Metrology to achieve the necessary traceability going from simple measurement methods, as using a Vernier caliper, to more precise and flexible methods, as three-dimensional coordinate measuring systems. For surface quality, the most common method is to make a roughness measurement with a surface roughness measuring machine (usually a 2D stylus instrument [14]). In many cases, manufacturers prefer to control texture and geometry without mechanical contact between the instrument and surface [15]. In addition, taking into account that one of the tendencies in AM processes is to reduce the size of the three-dimensional structures to micron size [4, 7], it is necessary to use other type of instruments. One of the most used nowadays, both in industry and in research, is confocal microscopy, which permits both dimensional and roughness measurements [16] without mechanical contact.

1.1. Confocal Microscopy

This type of microscope, developed in 1955 by M.L Minsky [17, 18], allows to obtain images of optical sections of the samples from which the full 3D geometry of the object can be reconstructed. The importance of confocal microscopy lies in being a powerful tool for observation and measurement both at scientific research level and at workshop level. It presents the following advantages [19]:

- The addition of the Z-axis to a traditional measuring optical microscopes which only work in the XY plane.
- It allows analyzing the 3D geometry of the object surface and characterize its quality from data points acquired while scanning it.
- The lateral resolution is better than in traditional optical microscopy.
- It permits to obtain more precise 3D images of the objects being measured, of higher quality and in shorter times compared to other methods. This allows to carry out many useful measurements in short intervals of time.
- Transparent specimens can be observed, as well as sections with a certain thickness, without no need to section the object under study.

Confocal microscopy has applications in many fields, both in research and in industrial applications. This type of microscope is widely used in biomedical science, material science and surface quality metrology at micro and macro-scale [20].

1.2. Operating Principle

Preprints (www.preprints.org) | NOT PEER-REVIEWED | Posted: 12 November 2019 doi:10.20944/preprints201911.0124.v1

Peer-reviewed version available at *Materials* **2019**, *12*, 4137; doi:10.3390/ma12244137

The confocal microscope usually uses a low power, high-intensity, monochromatic, laser system for illumination [21, 22, 23, 24]. Laser beam passes through a beam splitter and one of the beams is then redirected to the sample going through complex optics [18]. Once the scanning surface is illuminated, the reflected beam will travel the same way back. If the illumination is properly focused on the surface, the reflected beam will go to the detector without losing intensity, but if surface is out of focus, the intensity will be lower. The filtered beam arrives to the detector and a computer system processes the signal, making a 3D reconstruction of the surface [20, 21, 23].

Several factors affect the quality of these measurements [16, 25]:

- Metrological characteristics of the instrument: measurement noise, flatness deviation, linearity errors, amplification coefficients, squareness errors between axes and uniformity of the resolution of the measurements along the axis of operation.
- Instrument geometry: alignment of components and XY stage and rotary stage error motions.
- Source characteristics: focal spot size and drift.
- Detector characteristics: pixel response, uniformity and linearity, detector offset and bad pixels.
- Reconstruction and data processing: surface determinations, data representation and calculation approaches.
- Environmental conditions: Temperature, humidity and vibrations.

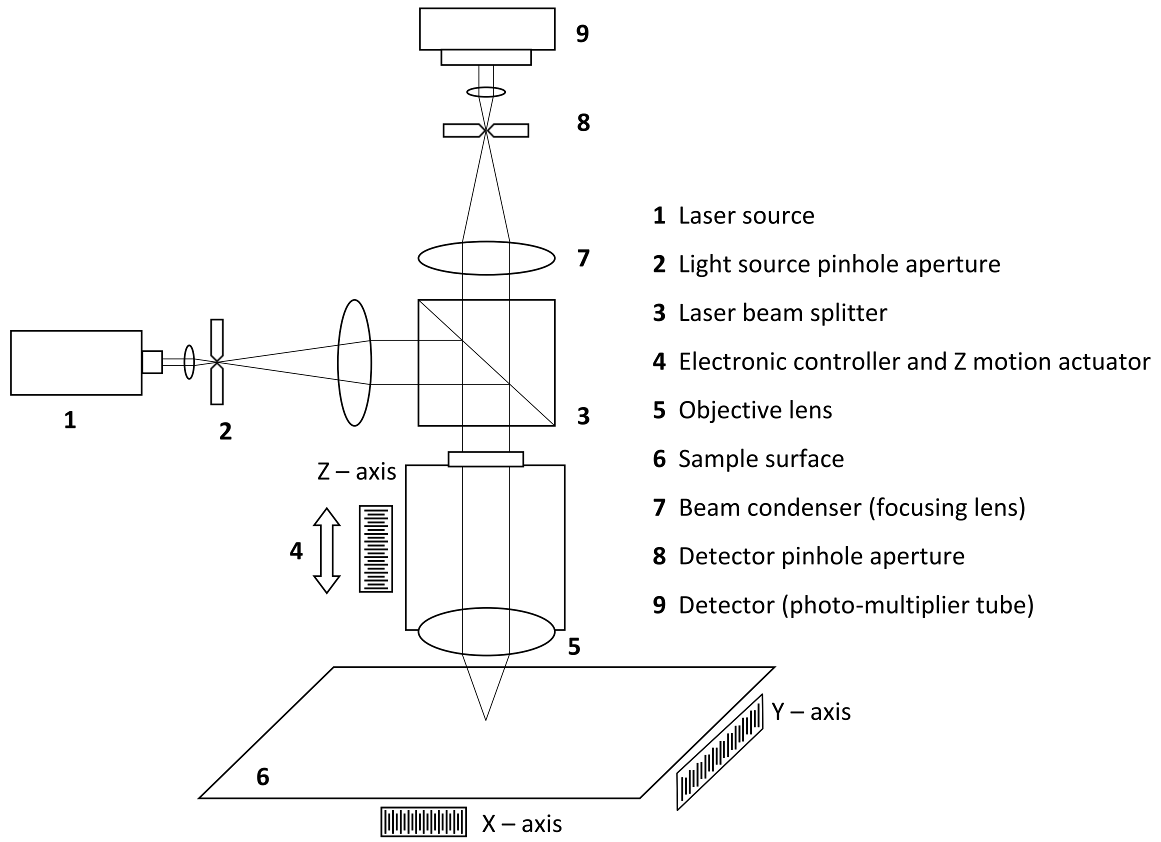

Figure 1. Scheme of a confocal microscopy [16, 23, 26].

The confocal microscope projects illumination patterns over the surface that is being explored and capture the returned rays through to the same pattern of illumination. As a result, it is possible to discriminate the returned rays that are out of focus and filter them [16, 18, 21, 22, 27].

Preprints (www.preprints.org) | NOT PEER-REVIEWED | Posted: 12 November 2019 doi:10.20944/preprints201911.0124.v1

Peer-reviewed version available at *Materials* **2019**, *12*, 4137; doi:10.3390/ma12244137

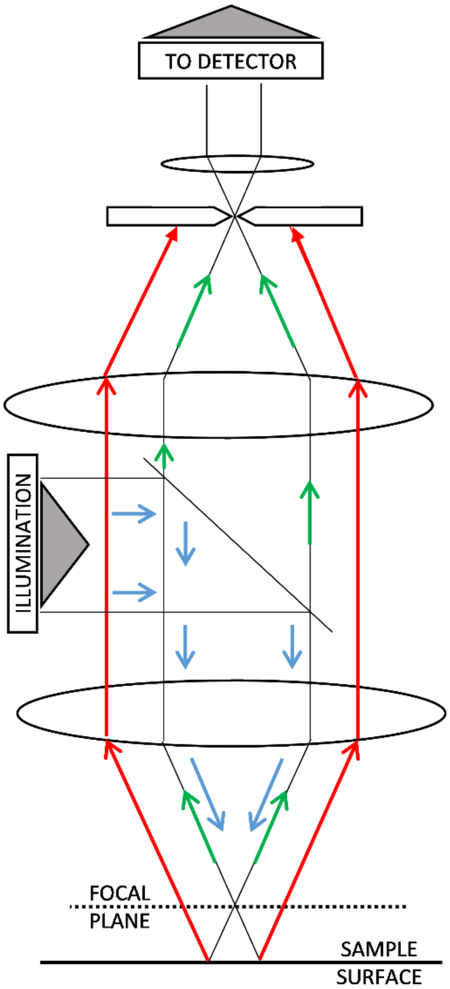

Figure 2. Filtration of out of focus signal (red) in confocal microscopy [16, 18, 21, 22, 27] in comparison with in focus signal (green).

Once the on focus image goes to the detector, the computational treatment starts. The electronic controller makes the confocal microscope able to take images at different steps along Z-axis. In this way, to make an interpolation between consecutive images to create the computational model of the scanned surface is needed. As in photography images are composed of pixels, the resolution of these models is measured by voxels. This concept allows discretizing the three-dimensional objects [28].

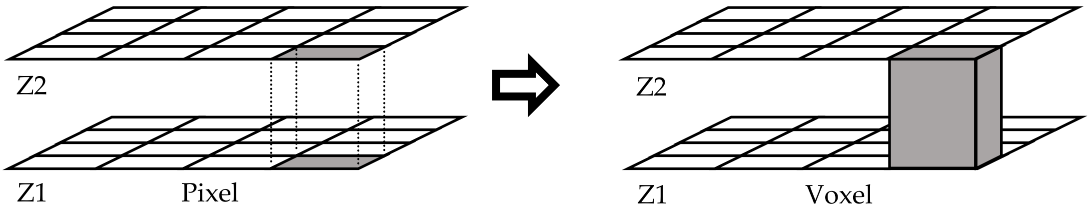

Figure 3. Transformation from pixel to voxel.

In order to achieve dimensional accuracy in measurements with confocal microscopy, it is important to know the size of the pixels, therefore it is necessary to make a dimensional calibration for X and Y-axes. Additionally, as our computerized model generates the voxels, it is necessary to know their height. For this reason, there is another scale that needs to be calibrated: the Z-axis.

The purpose of this paper is to describe how to provide suitable traceability to a confocal microscope when performing metrological activities in Additive Manufacturing using single topography measurements. The calibration procedures presented by the authors are intended to be simple and are based on classical mechanical standards. Please note that the objective is not to

Preprints (www.preprints.org) | NOT PEER-REVIEWED | Posted: 12 November 2019 doi:10.20944/preprints201911.0124.v1

Peer-reviewed version available at Materials 2019, 12, 4137; doi:10.3390/ma12244137

perform a state of the art calibration of a confocal microscope [29, 30, 31, 32], neither to achieve very low uncertainties, but just to ensure adequate traceability with adequate uncertainty estimation in the field of dimensional metrology for additive manufacturing. Please note that, when image stitching is not used (single topography) there is no movement of the XY stage and, therefore, there is no need to calibrate the displacements of this stage.

2. Materials and Methods

In order to ease the understanding of the calibration procedures described later in, the calibration will be carried to the following confocal microscope:

- Leica DCM3D confocal microscope with a 10× objective (EPI-L, NA 0,30). Field of view 1270 × 952 µm (768 × 576 pixels). 1,65 µm nominal voxel width. The overall range of the Z-axis is 944 µm using 2 µm axial steps (voxel height), but the instrument is used in a reduced working range of only 100 µm.
- SensoSCAN - LeicaSCAN DCM3D 3.41.0 software developed by Sensofar Tech Ltd.

The instrument is going to be used for single topography measurements, that is, without using image stitching. Therefore, XY stage is not moved during measurement and its errors do not contribute to uncertainty in single topography measurements.

The complete calibration procedure includes the following:

- Calibration of the X and Y scales, using a stage micrometer as a reference measurement standard.
- Estimation of the squareness error between X and Y-axes.
- Estimation of the flatness error of the focal plane using an optical flat.
- Calibration of Z scale using a calibrated steel sphere.
- Calibration of the confocal microscope for measurement of 2D roughness using periodic and aperiodic 2D roughness measurement standards.

- All uncertainties will b estimated following the mainstream GUM method (Guide to the Expression of Uncertainty in Measurement [33]) or EA-04/02 M:2013 document [34] as it is a standard procedure in calibration laboratories accredited under ISO 17025 [35].

All reference measurement standards used have been chosen to be:

- Easy to find.
- Easy to calibrate with low enough uncertainties in National Measurement Institutes (NMIs) or preferably in Accredited Calibration Laboratories (ACLs).
- Stable mechanical artifacts that could guarantee long re-calibration intervals
- Common in the field of dimensional metrology in order to facilitate its acquisition, calibration and correct use.

2.1. Flatness Calibration

Before calibrating the X and Y-axes, a flatness calibration must be performed. It is necessary because it is often observed that the XY plane of the confocal microscope is slightly curved. This is evident when exploring a flat surface such as an optical flat whose total flatness defects are usually lower than 50 nm. In these cases, the reference flat surface when observed by the confocal microscope appears curved, as if it was a cap of a sphere or an ellipsoid. According to manufacturers, this error is usually small enough but it is impossible to carry out an accurate measurement without taking into account this component of uncertainty [36].

For this calibration authors propose following a procedure based on [37], but using the confocal microscope instead of an interferometer. The software of confocal provides a topographic map of the explored surface from which the total flatness defect (peak to peak) or the RMS flatness defect can be estimated.

The calibration will be done in two positions (0° and 90°) and, therefore, two measurements will be obtained:

Peer-reviewed version available at *Materials* **2019**, *12*, 4137; doi:10.3390/ma12244137

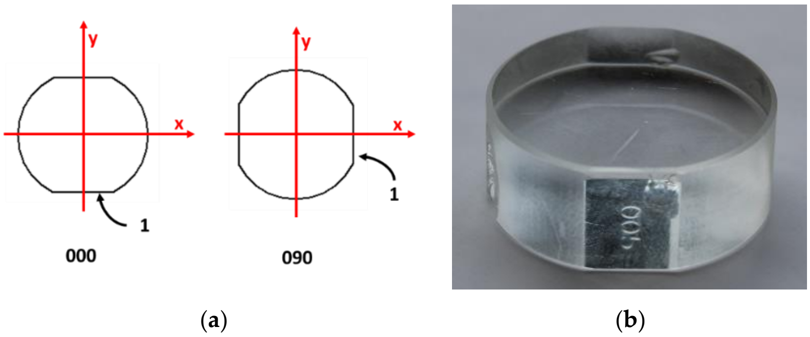

Figure 4. This figure shows (**a**) the different positions of scanning for the flatness pattern; (**b**) flatness pattern used during calibration.

For this calibration, authors recommend to use the RMS flatness defect because it is more statistically stable than the total flatness defect.

2.2. XY Plane Calibration

In the literature, it is possible to find several procedures for this calibration. Following the studies of de Vicente et al [38] and Guarneros et al [39] it is possible to calibrate scales X and Y and estimate their squareness error by making measurements of a stage micrometer in four positions:

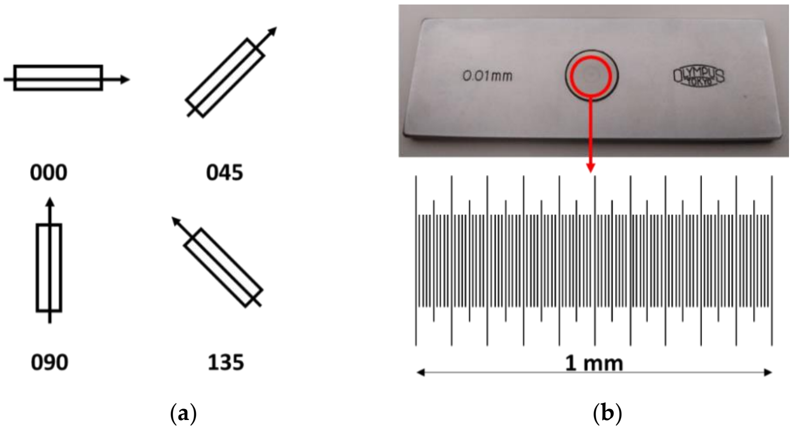

Figure 5. This figure shows (**a**) the different positions of scanning for the Stage Micrometer; (**b**) the stage micrometer used during calibration.

A stage micrometer is easy to calibrate in a National Measurement Institute (NMI) or in a accredited calibration laboratory (ACL) with uncertainty small enough (equal or lower than a 1 µm) for the calibration of a confocal microscope.

It is strongly recommended that the stage micrometer should be metallic and have the marks engraved, not painted, as those used to calibrate metallographic microscopes. Marks painted over glass are difficult to detect with a confocal instrument.

The matrix model proposed for calibration by de Vicente et al [40] would be the following:

$$\begin{bmatrix} x \\ y \end{bmatrix} = \begin{bmatrix} p \\ q \end{bmatrix} + \begin{bmatrix} c_{xy} + a & \theta/2 \\ \theta/2 & c_{xy} - a \end{bmatrix} \cdot \begin{bmatrix} p \\ q \end{bmatrix} \quad (1)$$

where (p, q) are the readings directly provided by the confocal microscope for the Cartesian coordinates in the XY plane. (x, y) are the corrected Cartesian coordinates once the calibration parameters c_{xy}, a and θ have been applied using the previous matrix model.

The meanings of these three parameters are the following:

- c_{xy} represents the deviation of actual pixel width w_{xy} from the nominal pixel width $w_{xy,nom}$:

$$w_{xy} = w_{xy,nom} \cdot (1 + c_{xy}) \quad (2)$$

Preprints (www.preprints.org) | NOT PEER-REVIEWED | Posted: 12 November 2019 doi:10.20944/preprints201911.0124.v1

Peer-reviewed version available at *Materials* **2019**, *12*, 4137; doi:10.3390/ma12244137

- a represents the difference between pixel widths along x-axis (w_x) and y-axis (w_y):

$$w_x = w_{xy,nom} \cdot \left(1 + c_{xy} + a\right) \tag{3}$$

$$w_y = w_{xy,nom} \cdot \left(1 + c_{xy} - a\right) \tag{4}$$

$$w_{xy} = \frac{(w_x + w_x)}{2} \tag{5}$$

- θ represents the squareness error between x-axis and y-axis. The actual angle between these axes is $\pi/2 - \theta$.

The amplification coefficients α_x, α_y and α_z of the axes (according to ISO 25178-70 [41]) would be:

$$\alpha_x = 1 + c_{xy} + a \tag{6}$$

$$\alpha_y = 1 + c_{xy} - a \tag{7}$$

$$\alpha_z = 1 + c_z \tag{8}$$

Authors recommend using the average pitch ℓ of the stage micrometers. ℓ would be the average of the all individual pitches (distances between two consecutive marks) observed in the images provided by the confocal microscope. Figure 6 summarize the measurement of the stage micrometer in one position. Using a special software for this task, it permits to estimate all distances between two consecutive marks (pitches) in the stage micrometers. Moreover, pitches can be measured in different positions: in the middle, in higher and in lower positions. In Figure 6a, for each pitch, the average value has been represented by a circle and the measurement variability around this value has been represented with a vertical line. In a similar way, non-linear errors have been depicted in Figure 6b.

(**a**)

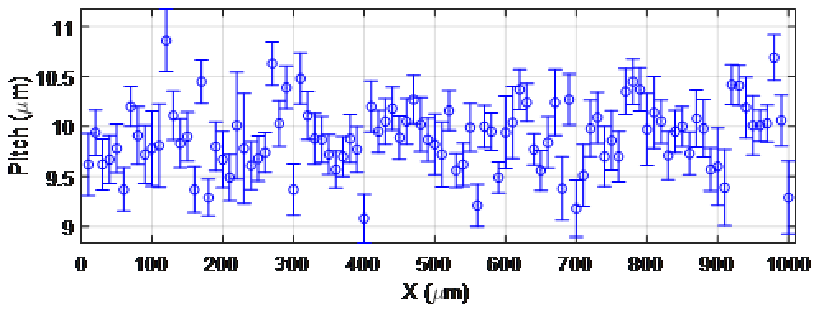

(**b**)

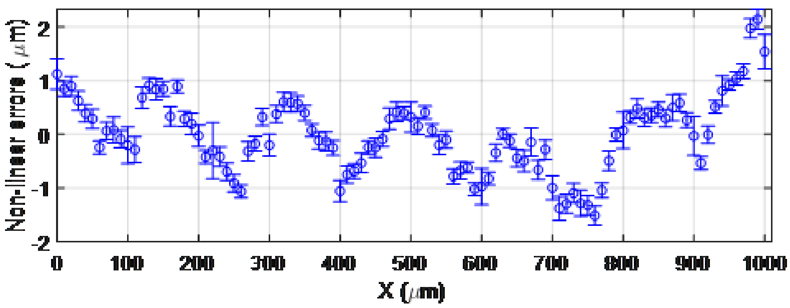

Figure 6. Measurement of stage micrometer in position 0°: (**a**) Pitch measurements results in μm (**b**) Non-linear errors in μm.

Let be ℓ_0 the average pitch of the stage micrometer certified by a suitable laboratory with a standard uncertainty $u(\ell_0)$. ℓ_1, ℓ_2, ℓ_3 and ℓ_4 are the average pitches measured with the confocal microscope in positions 0°, 90°, 45° and 135° respectively. Their corresponding standard uncertainties

Preprints (www.preprints.org) | NOT PEER-REVIEWED | Posted: 12 November 2019 doi:10.20944/preprints201911.0124.v1

Peer-reviewed version available at *Materials* **2019**, *12*, 4137; doi:10.3390/ma12244137

are $u(\ell_1)$, $u(\ell_2)$, $u(\ell_3)$ and $u(\ell_4)$ where only the variability observed in Figure 6 (or equivalent ones) has been taken into account.

When the matrix model is applied to positions 0°, 90°, 45° and 135° we obtain the following expressions which permit simple estimations of calibration parameters c_{xy}, a and θ:

$$\text{Position } 0°: \quad \ell_1 \cdot (1 + c_{xy} + a) \cong \ell_0 \tag{9}$$

$$\text{Position } 90°: \quad \ell_2 \cdot (1 + c_{xy} - a) \cong \ell_0 \tag{10}$$

$$\text{Position } 45°: \quad \ell_3 \cdot (1 + c_{xy} + \theta/2) \cong \ell_0 \tag{11}$$

$$\text{Position } 135°: \quad \ell_4 \cdot (1 + c_{xy} - \theta/2) \cong \ell_0 \tag{12}$$

From those expressions it is easy to conclude that possible estimations of c_{xy}, a and θ are:

$$c_{xy} = \frac{\ell_0}{4} \cdot \left(\frac{1}{\ell_1} + \frac{1}{\ell_2} + \frac{1}{\ell_3} + \frac{1}{\ell_4}\right) - 1 \tag{13}$$

$$\text{with } u(c_{xy}) = \frac{\sqrt{u^2(\ell_0) + [u^2(\ell_1) + u^2(\ell_2) + u^2(\ell_3) + u^2(\ell_4)]/16}}{\ell_0} \tag{14}$$

$$a = \frac{\ell_0}{2} \cdot \left(\frac{1}{\ell_1} - \frac{1}{\ell_2}\right) \tag{15}$$

$$\text{with } u(a) = \frac{\sqrt{u^2(\ell_1) + u^2(\ell_2)}}{2\ell_0} \tag{16}$$

- $$\theta = \ell_0 \cdot \left(\frac{1}{\ell_3} - \frac{1}{\ell_4}\right) \tag{17}$$

$$\text{with } u(\theta) = \frac{\sqrt{u^2(\ell_3) + u^2(\ell_4)}}{\ell_0} \tag{18}$$

Correlations between these parameters (c_{xy}, a and θ) are usually very small (lower than 0,01). Therefore, these correlations can be neglected.

2.3. Z-Axis Calibration

Document [42] propose calibrating the Z-axis to use a step gauge build with gauge blocks over an optical flat. However, the short field of view of a confocal microscope makes it difficult to carry out the calibration with this type of measurement standards.

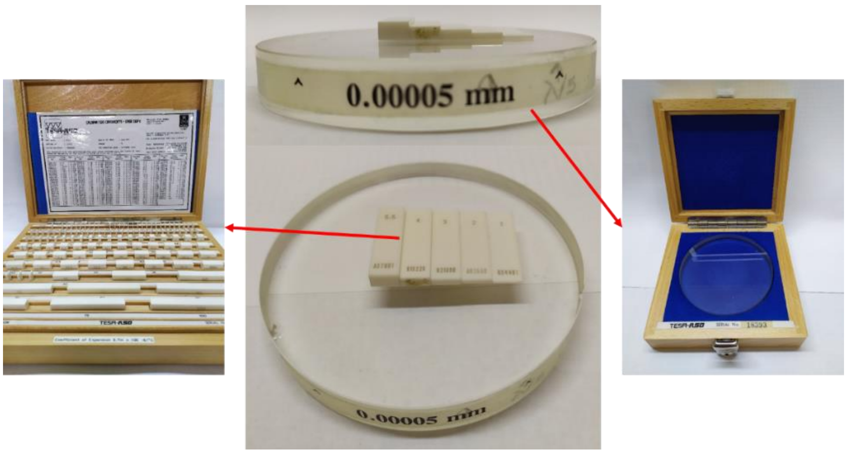

Figure 7. A step gauge build with an optical flat and gauge blocks.

To solve this problem, several authors [16, 43] propose to use step height standards. Wang et al [43] used them with nominal values 24, 7, 2 and 0,7 µm. This kind of measurement standards have

Preprints (www.preprints.org) | NOT PEER-REVIEWED | Posted: 12 November 2019 doi:10.20944/preprints201911.0124.v1

Peer-reviewed version available at *Materials* **2019**, *12*, 4137; doi:10.3390/ma12244137

several grooves whose nominal depths cover the range of use of the confocal microscope on the Z-axis. Following their procedures, every groove has to be measured ten times, changing the position of the standard on the objective.

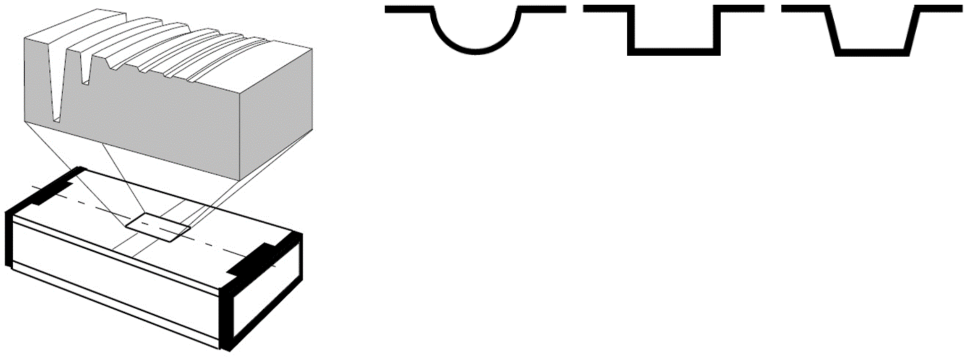

(**a**) (**b**)

Figure 8. This figure shows (**a**) a typical model of step height standard and (**b**) different models of step height standards grooves (ISO 5436-1 types A and B). [38, 43, 44, 45]

This kind of standard is typically used for roughness calibration. If the purpose is to make a calibration on Z-axis, these standards have the limitation of the groove's depth, which usually is small to cover the range of the Z-axis.

In order to solve this problem, authors propose using a small metallic sphere with nominal diameter between 1 mm and 10 mm, similar to the one used in [46]. This kind of measurement standard is easy to find and easy to calibrate both in NMIs or in ACLs with uncertainties equal or lower than 0,5 µm. The software of the confocal microscope permits to fit a spherical surface to the points detected over the observed surface of the spherical measurement standard. Therefore, it is possible to compare the certified diameter D_0 of the sphere against the diameter D_m of the spherical surface fitted by the confocal microscope. Authors propose to use an extended matrix model to take into account the calibration of the Z-axis:

$$\begin{bmatrix} x \\ y \\ z \end{bmatrix} = \begin{bmatrix} p \\ q \\ r \end{bmatrix} + \begin{bmatrix} 1 + c_{xy} + a & \theta/2 & 0 \\ \theta/2 & 1 + c_{xy} - a & 0 \\ 0 & 0 & 1 + c_z \end{bmatrix} \cdot \begin{bmatrix} p \\ q \\ r \end{bmatrix} \tag{19}$$

Where p, q, r are readings provided by the confocal microscope for the Cartesian coordinates x, y, z. The calibration parameters are those described in section 2.2 (c_{xy}, a, θ) and the new parameter c_z is introduced to permit the calibration in Z-axis. The corrected z coordinate would be:

$$z = (1 + c_z) \cdot r \tag{20}$$

This simple matrix model supposes that there is no perpendicular error (or it is negligible) between Z-axis and XY-plane. This a hypothesis very close to reality when the Z-axis range is clearly lower than ranges of X and Y-axes. When Z-axis range is equal or higher than X, Y ranges a more complex model must be used (zero terms in the matrix of the model are no longer zero, see, for example the document [47]). It is easy to demonstrate that, using the matrix model, the corrected diameter D of the spherical surface fitted by the confocal microscope software would be:

$$D = D_m \cdot \frac{1 + 2c_{xy}}{1 + c_z} \tag{21}$$

Where D_m is the diameter provided by the confocal microscope prior to apply any calibration parameter. Therefore an estimation of c_z would be:

$$c_z = \frac{D_m}{D_0} \cdot (1 + 2c_{xy}) - 1 \tag{22}$$

Preprints (www.preprints.org) | NOT PEER-REVIEWED | Posted: 12 November 2019 doi:10.20944/preprints201911.0124.v1

Peer-reviewed version available at Materials 2019, 12, 4137; doi:10.3390/ma12244137

Where D_0 is the certified diameter of the sphere by the ACL. The standard uncertainty of c_z would be:

$$u(c_z) = \sqrt{\frac{u^2(D_0) + u^2(D_m)}{D_0^2} + 4u^2(c_{xy})} \tag{23}$$

The expression (22) of c_z shows a clear positive dependency with c_{xy}. Therefore, the correlation coefficient $r(c_z, c_{xy})$ should be estimated and it can be done using the following expression:

$$r(c_z, c_{xy}) = 2 \cdot \frac{u(c_{xy})}{u(c_z)} \tag{24}$$

Figure 9. Steel sphere used in calibration.

2.4 Calibration for Roughness Measurements

The calibration of Z-axis against the reference sphere (previous section) guarantees the traceability of the vertical measurements performed with the confocal microscope to the SI unit of length (the meter). Therefore, any vertical roughness parameter will have an adequate traceability once the instrument has been calibrated along its Z-axes. Notwithstanding, authors followed the recommendation included in documents DKD-R 4-2 [48, 49, 50] which propose to perform an additional calibration against roughness standards to validate the Z-axis calibration for roughness measurements.

There are many parameters used to characterize surface texture. Among 2D roughness parameters, one of the most widely used is the R_a parameter, which is the arithmetic mean of the absolute values of the profile deviations from the mean line of the roughness profile [51]. Authors will only consider the R_a parameter during calibration, but readers interested in other 2D roughness vertical parameters (R_q, R_p, R_v, R_z, …) can use the same calibration procedure described in this paper but only with minor variations. Calibration will be performed in the range $0{,}1\ \mu m < R_a \leq 2\ \mu m$. For this range, according to ISO 4288 [52], the sampling length should be l_r = 0,8 mm, which is possible to carry out with a field of view of 1270 × 952 µm. For $R_a > 2\ \mu m$ the sampling length should be l_r = 2,5 mm or higher and it is impossible to achieve it with a field of view of 1270 × 952 µm (10× objective). Measuring roughness lower than $R_a = 0{,}1\ \mu m$ has no sense with an instrument with repeatability in Z-axis around 0,5 µm. Therefore, calibration for $R_a < 0{,}1\ \mu m$ and $R_a > 2\ \mu m$ is discarded.

Figure 10a shows three metallic, aperiodic 2D roughness standards. Figure 10b shows three glass, periodic 2D roughness standards. Other types of 2D roughness profile types are described in section 7 of ISO 25178-70 [41]. Authors recommend the use of aperiodic standards because they cover a wide range of wavelengths in contrast to periodic standards that only cover a single wavelength. However, periodic standards will be used in this case in order to complete the range of measurements between 0,1 µm and 2 µm for different calibration points and for different materials (glass instead of metallic items).

Preprints (www.preprints.org) | NOT PEER-REVIEWED | Posted: 12 November 2019 doi:10.20944/preprints201911.0124.v1

Peer-reviewed version available at *Materials* **2019**, *12*, 4137; doi:10.3390/ma12244137

(**a**) (**b**)

Figure 10. Step height standards used during calibration. (**a**) aperiodic, metallic standards (**b**) periodical, glass standards.

These standards will be measured over five different zones in two different orientations (see Figure 11a,b). In each zone, the measurement is carried out along a line always perpendicular to the roughness lines (see Figure 11c) and located at the center of the zone. Therefore, a total of $2 \cdot 5 = 10$ roughness measurements will be obtained from each standard.

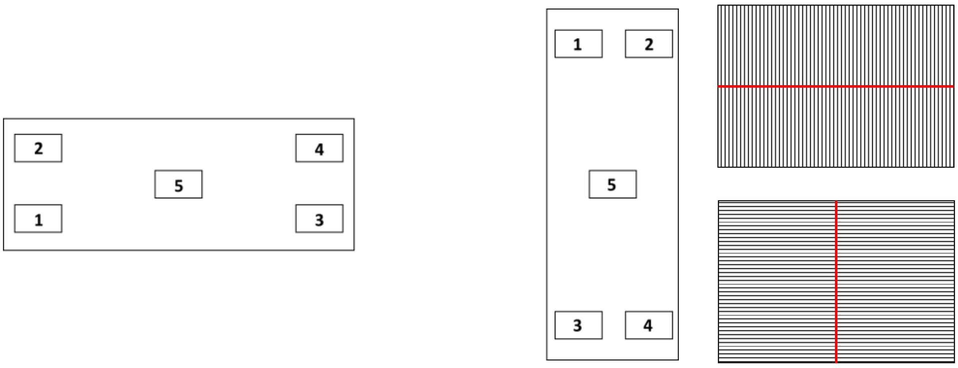

(**a**) (**b**) (**c**)

Figure 11. Location of the five scanning position for roughness calibration: (**a**) horizontal orientation; (**b**) vertical orientation and (**c**) location of measurement lines

Authors recommend to use, at least, three different roughness standards with nominal values of R_a uniformly distributed along the range where the instrument must be calibrated. However, it is advisable to use five or more standards and, if possible, made of different materials, for example, metallic and glass.

It is important to note that there will be differences between measurements obtained with a confocal microscope and measurements obtained with a stylus instrument [53, 54]. Main reasons for that are:

- The way the surface is detected is totally different: microscopes use light and stylus instruments a mechanical tip. As a consequence, optical instruments tend to overestimate surface roughness.
- Stylus instruments permit evaluation lengths l_n as long as necessary (see ISO 4288 [52]). Microscopes usually have small fields of view that limit the maximum length of the profile that can be scanned. For example, for samples with 0,1 μm < R_a ≤ 2 μm, ISO 4288 recommends using five sampling lengths l_r = 0,8 mm for a total evaluation length l_n = 4 mm. This is not a problem at all for stylus instruments, which can cope with longer evaluation lengths (up to 100 mm in some cases). But the confocal microscope described at the beginning of section 2 has a maximum evaluation length of 1,27 mm. Therefore, only one sampling length l_r = 0,8 mm can be used. Using only one sampling length instead of five usually causes a bias towards lower R_a accompanied by an increase in variability. The effect is considerably higher when even the sampling length l_r has to be reduced.

Preprints (www.preprints.org) | NOT PEER-REVIEWED | Posted: 12 November 2019 doi:10.20944/preprints201911.0124.v1

Peer-reviewed version available at *Materials* **2019**, *12*, 4137; doi:10.3390/ma12244137

In order to ensure a good match between roughness measurement performed with stylus instruments and optical instruments, the concept of "bandwidth matching" should be correctly applied [53].

2.5. Summary of Characteristics of Measurement Standards Used during Calibration

In this section, the nominal values and the uncertainties of the different measurement standards used during calibration are summarized. All of them were calibrated in ACLs.

Table 1. Nominal values and the uncertainties of the material reference standards used during calibration. [1] S_m is a spacing parameter defined as the mean spacing between peaks. S_m values included in this table are only informative.

Reference Measurement Std.	Parameter	Certified Value (µm)	Std. Uncertainty (k = 1) (µm)
Optical flat	Total flatness defect	0,118	0,025
	RMS flatness defect	0,028	0,007
Stage Micrometer	Average pitch ℓ_0	9,980	0,005
Sphere	Diameter D_o	4 001,08	0,25
Roughness std. #1 metallic, aperiodic	R_a (R_0)	0,183	0,039
	S_m [1]	48	
Roughness std. #2 metallic, aperiodic	R_a (R_0)	0,512	0,041
	S_m [1]	185	
Roughness std. #3 metallic, aperiodic	R_a (R_0)	1,677	0,057
	S_m [1]	176	
Roughness std. #4 glass, periodic	R_a (R_0)	0,460	0,030
	S_m [1]	100	
Roughness std. #5 metallic, aperiodic	R_a (R_0)	0,850	0,030
	S_m [1]	120	
Roughness std. #6 glass, periodic	R_a (R_0)	2,440	0,080
	S_m [1]	200	

We include the calibration of the confocal microscope against roughness standard #6 only for informative purposes. Its measurements were made using a sampling length l_r = 0,8 mm because of the reduced field of view of the instrument (with an ×10 objective). However, according to ISO 4288 [52], it is recommended to use a sampling length l_r = 2,5 mm, measurement impossible to achieve with a ×10 objective.

3. Results

3.1. Flatness Calibration

The following figure shows a topographic image of the optical flat of Figure 4 that has been used as a flatness calibration surface. This optical flat has been calibrated previously in an accredited laboratory. Total flatness defect is 118 nm with a standard uncertainty of 25 nm (k = 1) and its RMS flatness defect is 28 nm with a standard uncertainty of 7 nm (k = 1), see Table 1.

Preprints (www.preprints.org) | NOT PEER-REVIEWED | Posted: 12 November 2019 doi:10.20944/preprints201911.0124.v1

Peer-reviewed version available at *Materials* **2019**, *12*, 4137; doi:10.3390/ma12244137

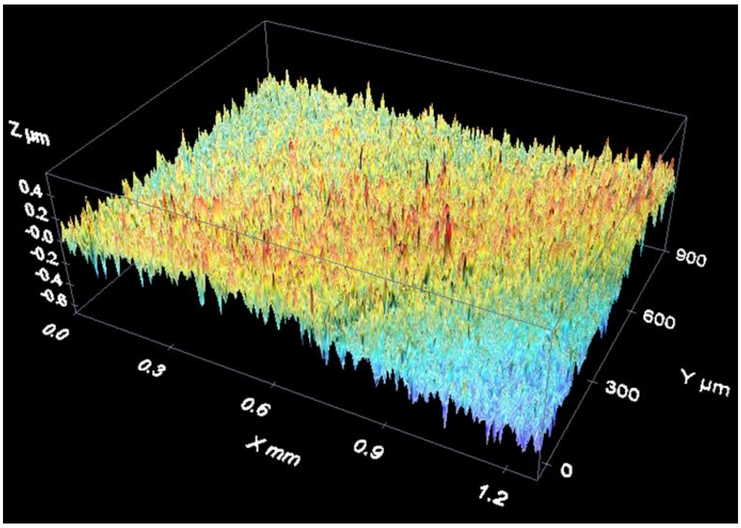

Figure 12. Result of the glass flatness pattern measurement.

Figure 12 shows the absence of visible curvature in the XY plane. It could be an empirical demonstration of a good adjustment and/or correction of the microscope by the manufacturer. In a situation like this there is no need to apply any correction to compensate the curvature of the XY-plane.

Table 2 shows the results of the measurements performed with the confocal microscope (in both positions 0° and 90°):

Table 2. RMS flatness defect measured with the confocal microscope in positions 0º and 90º.

Position	RMS value (µm)
0°	0,48
90°	0,59

The RMS values of Table 2 are small values when compared with Z-axis axial step (2,0 µm). Therefore, they are probably caused only by the lack of repeatability of the instrument. In any case, the most conservative option is to estimate a component of the uncertainty associated with the possible curvature of the XY plane equal to the average value of both RMS values of Table 2:

$$u_{\mathrm{FLT}} = 0{,}54\ \ \mu\mathrm{m} \tag{25}$$

Probably a better estimation for u_{FLT} would be to subtract quadratically the RMS flatness of the optical flat (0,28 µm):

$$u_{\mathrm{FLT}} = \sqrt{(0{,}54\ \mu\mathrm{m})^2 - (0{,}028\ \mu\mathrm{m})^2} = 0{,}539\ \mu\mathrm{m} \tag{26}$$

Anyway, authors consider that the first estimation ($u_{\mathrm{FLT}} = 0{,}54$ µm) is slightly more conservative and clearly simpler.

3.2. XY Plane Calibration

The following figure shows the four positions (0°, 90°, 45°, 135°) in which the stage micrometer was measured in the confocal microscope during de XY plane calibration:

Peer-reviewed version available at *Materials* **2019**, *12*, 4137; doi:10.3390/ma12244137

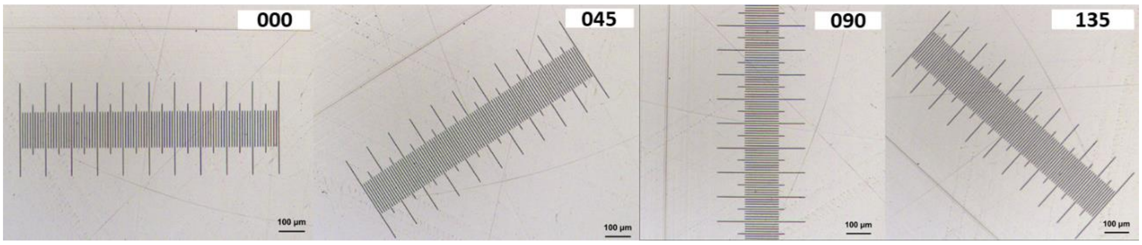

Figure 13. Different measurement positions (0°, 90°, 45°, 135°) of stage micrometer.

In each position, the average pitch ℓ_i was determined from the readings provided by the confocal microscope. The results are shown in Table 3.

Table 3. Measurements of the middle step, the standard deviation and the uncertainty of the measurements of stage pattern.

Position	Average Pitch ℓ_i(µm)	Uncertainty $u(\ell_i)$ (µm)	Repeatability s (µm)	Non Linearity RMS (µm)
1- 0°	9,892 34	0,000 53	0,34	0,71
2- 90°	9,891 56	0,000 49	0,42	0,69
3- 45°	9,897 33	0,000 57	0,38	0,60
4- 135°	9,889 50	0,000 47	0,34	0,61

An average value for repeatability in XY plane would be $s_r(x) = s_r(y) = 0{,}4$ µm. It is a reasonable value when compared with 1,65 µm lateral resolution (nominal voxel width).

The stage micrometer has a certified average pitch $\ell_0 = 9{,}980$ µm with a standard uncertainty $u(\ell_0) = 0{,}005$ µm.

Using expression for section 2.2 we obtain the following estimations for calibration parameters c_{xy}, a and:

$$c_{xy} = \frac{\ell_0}{4} \cdot \left(\frac{1}{\ell_1} + \frac{1}{\ell_2} + \frac{1}{\ell_3} + \frac{1}{\ell_4}\right) - 1 = 0{,}008\ 83 \tag{27}$$

$$\text{with } u(c_{xy}) = \frac{\sqrt{u^2(\ell_0) + [u^2(\ell_1) + u^2(\ell_2) + u^2(\ell_3) + u^2(\ell_4)]/16}}{\ell_0} = 0{,}000\ 50 \tag{28}$$

$$a = \frac{\ell_0}{2} \cdot \left(\frac{1}{\ell_1} - \frac{1}{\ell_2}\right) = -0{,}000\ 040 \tag{29}$$

$$\text{with } u(a) = \frac{\sqrt{u^2(\ell_1) + u^2(\ell_2)}}{2\ell_0} = 0{,}000\ 036 \tag{30}$$

$$\theta = \ell_0 \cdot \left(\frac{1}{\ell_3} - \frac{1}{\ell_4}\right) = -0{,}000\ 798 \tag{31}$$

$$\text{with } u(\theta) = \frac{\sqrt{u^2(\ell_3) + u^2(\ell_4)}}{\ell_0} = 0{,}000\ 074 \tag{32}$$

All three parameters are dimensionless.

Observing non-linearity RMS values in Table 3, an overall standard uncertainty estimation for non-linearity in the XY-plane would be $u_{\mathrm{NL},xy} = 0{,}7$ µm.

3.3. Z-Axis Calibration

Figure 14 shows an example of a measurement of a spherical cap of a stainless steel reference sphere with a 4 mm nominal diameter (see Figure 9). It is a three-dimensional reconstruction of the sphere surface.

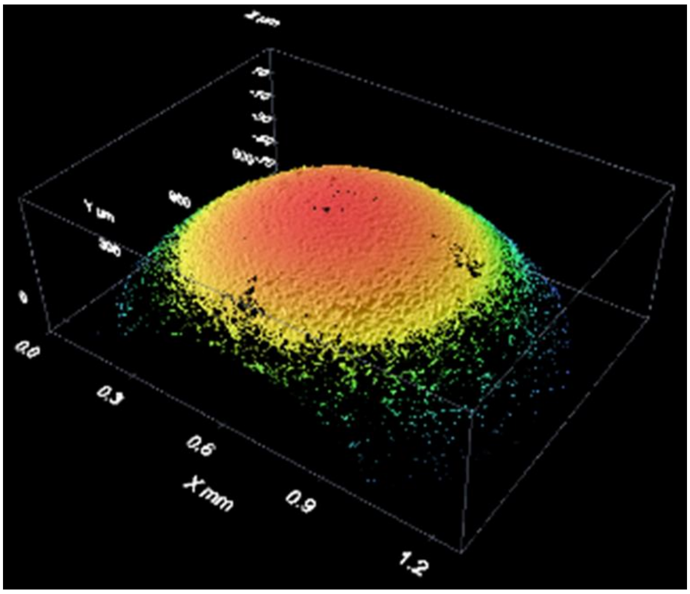

Figure 14. This figure shows the results of the measurement of the bearing sphere with white light.

Using this information, the confocal microscope software can perform a least-square fitting to a spherical surface from which we can estimate the diameter of the sphere and RMS error of the fit.

In this calibration, two different types of illumination are used (white and blue light) and measurements were taken in three orientations: 0°, 45° and 90°. Finally, there are $n = 6$ measurements.

Table 4. Root-mean-square error, diameter D_m and standard deviation $u(D_m)$ of the spherical caps fitted using least-squares.

Position	Illumination	RMS error (µm)	Diameter D_m (mm)
0°	Blue	0,86	3,9740
45°	Blue	1,08	3,9562
90°	Blue	1,08	3,9638
0°	White	0,86	3,9740
45°	White	0,89	3,9828
90°	White	0,87	3,9766

The average value $\overline{D}_m$ of the six diameters D_m is $\overline{D}_m$ = 3.9712 mm and the standard deviation $s(D_m)$ = 0,0096 mm. We will estimate $u(\overline{D}_m)$ as:

$$u(\overline{D}_m) = \frac{s(D_m)}{\sqrt{n}} = 0{,}0039 \text{ mm} \tag{33}$$

The RMS error is an estimation of the repeatability in the Z-axis that, probably, includes to the non-linearity in the Z-axis. A mean value for this Z-axis repeatability would be $s_r(z)$ = 0,8 µm which seems to be a resasonable value when compared with the Z-axis axial step of 2 µm.

The certified diameter D_0 of the reference sphere is D_0 =4,00 01 mm with a standard uncertainty $u(D_0)$ = 0,25 µm.

Using the expression of section 2.3 the Z-axis calibration parameter c_z can be estimated as follows:

$$c_z = \frac{D_m}{D_0} \cdot \left(1 + 2c_{xy}\right) - 1 = 0{,}0101 \tag{34}$$

$$\text{with } u(c_z) = \sqrt{\frac{u^2(D_0)+u^2(\bar{D}_m)}{D_0^2} + 4u^2(c_{xy})} = 0{,}0014 \tag{35}$$

The correlation coefficient $r(c_z, c_{xy})$ would be:

$$r(c_z, c_{xy}) = 2 \cdot \frac{u(c_{xy})}{u(c_z)} = 0{,}72 \tag{36}$$

This correlation coefficient is clearly higher than zero showing a strong positive correlation between c_z and c_{xy} that should be taken into account after calibration when needed.

Correlation coefficients $r(c_z, a)$ and $r(c_z, \theta)$ are usually very small (lower than 0,01) and therefore correlation between c_z and parameters a and θ can be neglected.

3.4. Calibration for Roughness Measurements

As an example of data acquisition results when measuring a material roughness standard, the following figures show three-dimensional reconstructions of the surface of an aperiodic, metallic roughness standard (Figure 15) and a periodic, glass roughness standard (Figure 16).

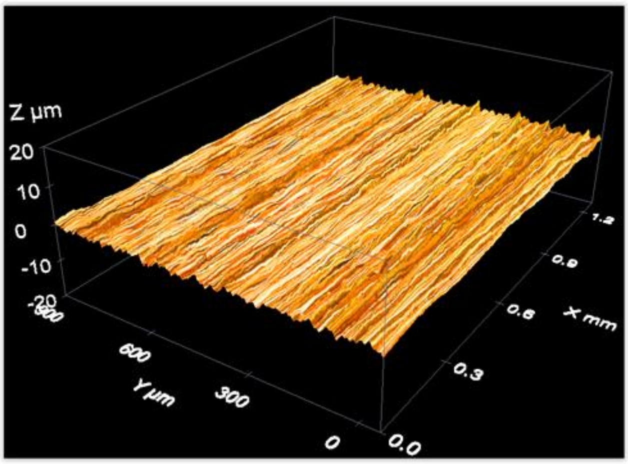

Figure 15. Measurement of an aperiodic roughness standard with a confocal microscope: a 3D view of the measurement results.

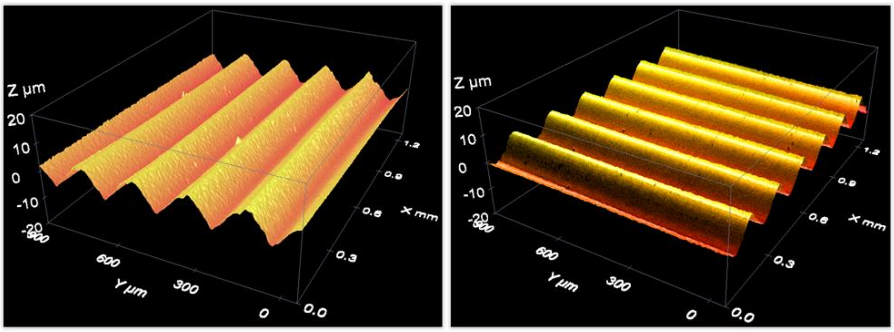

(**a**) (**b**)

Figure 16. Measurement of a periodic roughness standard with a confocal microscope: a 3D view of the measurement results with roughness lines in (**a**) parallel to X-axis and in (**b**) parallel to Y-axis.

Calibration is performed by repeating $10 = 5 \cdot 2$ times (five zones, two orientations) the measurements of six roughness standards (see Table 1). Results are summarized in Table 5: average results $\bar{R}$ of the ten repeated measurements and its corresponding standard deviations $s(R)$. Direct

Preprints (www.preprints.org) | NOT PEER-REVIEWED | Posted: 12 November 2019 doi:10.20944/preprints201911.0124.v1

Peer-reviewed version available at Materials 2019, 12, 4137; doi:10.3390/ma12244137

readings R provided by the confocal microscope were obtained prior to introduced the calibration parameter c_z using only one sampling length $l_r = 0{,}8$ mm.

Therefore, these readings should be correcting applying the following expression to take into account the Z-axis calibration:

$$R_{\text{corrected}} = \bar{R} \cdot (1 + c_z) \tag{37}$$

Authors followed the recommendations of ISO 4288 [52] that, for $0{,}1\ \text{mm} < R_a \leq 2\ \text{mm}$, recommend five sampling length $l_r = 0{,}8$ mm for a total evaluation length of $l_n = 4$ mm. Due to the limitations of the field of view of the instrument, (see section 2) only one sampling length $l_r = 0{,}8$ mm could be used. This reduction in the number of sampling lengths from five to one would cause slightly lower values for R_a and higher variabilities [53].

Table 5. Results obtained when calibrating the confocal microscope described in section 2 using six roughness standards (Table 1). [1] Values obtained when measuring roughness standard #6 are included in this table only by informative reasons. Measurements of this standard were made using a sampling length $l_r = 0{,}8$ mm, because of the reduced field of view of the instrument, instead of a sampling length $l_r = 2{,}5$ mm as recommended by ISO 4288 [52].

Reference Meas. Std.	Average R_a $\bar{R}$ (µm)	Repeatability $s(R)$ (µm)	Corrected R_a $\bar{R} \cdot (1 + c_z)$ (µm)	Bias estimation b (µm)	Standard Uncertainty $u(b)$ (µm)
Roughness std. #1	0,43	0,06	0,43	0,25	0,04
Roughness std. #2	0,59	0,06	0,60	0,08	0,05
Roughness std. #3	1,70	0,11	1,71	0,04	0,07
Roughness std. #4	0,51	0,04	0,52	0,06	0,03
Roughness std. #5	0,95	0,05	0,96	0,11	0,03
Roughness std. #6 [1]	2,50	0,06	2,53	0,09	0,08

It can be concluded from Table 5 that a typical value for $s(R)$ would be $s(R) = 0{,}07$ µm, the quadratic average of repeatabilities of the first five standards.

Note that corrected values $\bar{R} \cdot (1 + c_z)$ are always higher than the certified values R_0 (compare results from Table 5 to those from Table 1). It seems that for surface roughness similar to the nominal voxel height ($w_z = 2$ µm) readings provided by the confocal microscope present a positive bias caused by noise observed, for example, when measuring an optical flat (see section 3.1, Figure 12). The RMS flatness error observed when measuring the optical flat (0,54 µm) is slightly higher than R_a observed when measuring roughness std. #1, a quasi-flat surface (certified value $R_a = 0{,}183$ µm) for an instrument with a voxel height of 2 µm. Definition of R_a is similar but not equal to definition of RMS flatness but, most important, R_a is evaluated after filtering the readings using a low-pass filter (defined through the sampling length l_r).

Authors suggest to estimate the positive bias at each calibration point using the following expression, where R_0 is R_a certified value for the standard used at each calibration point:

$$b = \bar{R} \cdot (1 + c_z) - R_0 \tag{38}$$

Its corresponding standard uncertainty $u(b)$ would be:

$$u(b) = \sqrt{u^2(R_0) + \bar{R}^2 \cdot u^2(c_z) + \frac{s^2(R)}{n}} \tag{39}$$

Preprints (www.preprints.org) | NOT PEER-REVIEWED | Posted: 12 November 2019 doi:10.20944/preprints201911.0124.v1

Peer-reviewed version available at Materials 2019, 12, 4137; doi:10.3390/ma12244137

Using this approach, the calibration results are those values, b_i and $u(b_i)$, presented in the two columns on the right side of Table 5. Index i refers to the roughness standard used. These results have been represented graphically in figure 17. Red lines represent values corresponding to metallic, aperiodic standards #1, #2 and #3. Green lines represent values corresponding to standards #4 and #5. The blue line is the result from standard #6 that will not be taken into account. Vertical lines represents uncertainty intervals $b_i \pm U(b_i)$ where the expanded uncertainties $U(b_i) = k \cdot u(\bar{b})$ has been evaluated for $k = 2$. The horizontal black solid line corresponds to the average value $\bar{b}$ of the first $N = 5$ roughness standards:

$$\bar{b} = \frac{\sum_{i=1}^{N} b_i}{N} = \frac{b_1 + b_2 + b_3 + b_4 + b_5}{5} = 0{,}11\ \mu\text{m} \tag{40}$$

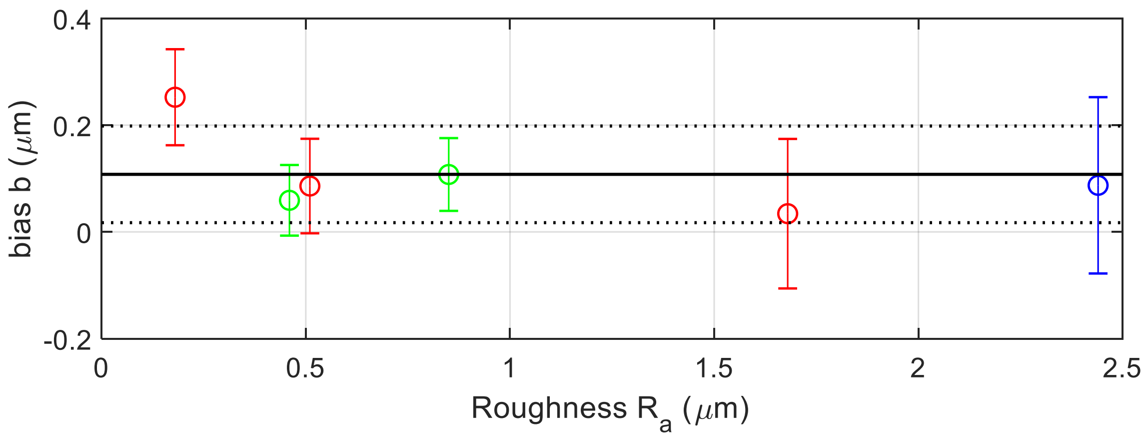

Figure 17. Bias observed at each calibration point (roughness calibration).

In order to make a correct estimation of average bias$\bar{b}$, correlation between bias b_i at each calibration points should be taken into account. Due to these facts:

- Dominant contributions to uncertainties $u(b_i)$ are the calibration uncertainties $u(R_0)$ of the roughness standards.
- There is a high probability that all roughness standards have been calibrated in the same calibration laboratory. Therefore, there will be strong correlation between them.

There will be a high correlation between bias b_i. Authors have performed estimations in different situations and it is possible to see correlation coefficients $r(b_i, b_j)$ as high as +0.8.

In order to simplify calculations authors suggest assuming $r(b_i, b_j) = +1$, which leads to higher estimations for the uncertainty $u(\bar{b})$ of $\bar{b}$. Then, it can be demonstrated that $u(\bar{b})$ is:

$$u(\bar{b}) = \frac{1}{N}\sum_{i=1}^{N} u(b_i) = \frac{u(b_1) + u(b_2) + u(b_3) + u(b_4) + u(b_5)}{5} = 0{,}05\ \mu\text{m} \tag{41}$$

In Figure 17, the uncertainty interval $\bar{b} \pm U(\bar{b})$ is represented by the space between the higher and lower black dotted lines. $U(\bar{b}) = k \cdot u(\bar{b})$ is the expanded uncertainty of $\bar{b}$ evaluated with a coverage factor $k = 2$. Please note that all uncertainty intervals $b_i \pm U(b_i)$ overlap the interval $\bar{b} \pm U(\bar{b})$. Notwithstanding, point b_1 is outside the interval $\bar{b} \pm U(\bar{b})$. This could indicate that some variability of the bias b has not been taken into account in $u(\bar{b})$. Therefore, a conservative approach would be to assume that there is a variability represented by δb that should be added to $u(\bar{b})$. Let suppose that δb is a uniform random variable of null mean and a full range $b_{\max} - b_{\min}$. Then its standard uncertainty would be:

$$u(\delta b) = \frac{b_{\max} - b_{\min}}{\sqrt{12}} = 0{,}06\ \mu\text{m} \tag{42}$$

Preprints (www.preprints.org) | NOT PEER-REVIEWED | Posted: 12 November 2019 doi:10.20944/preprints201911.0124.v1

Peer-reviewed version available at Materials 2019, 12, 4137; doi:10.3390/ma12244137

In order to estimate the noise of the instrument, according to documents [48, 49, 50], we repeat ten measurements over a on optical flat (that of Figure 4) in two orientation: 0º and 90º. An optical flat is, for a confocal microscope, a specimen with null roughness (very small in comparison with its noise). Therefore, values of R_a obtained over an optical flat are a very good estimation of the instrument noise. The average value and the standard deviation of the ten R_a values were:

$$\bar{R}_a = 0{,}09\ \mu\text{m} \tag{43}$$

$$s(R_a) = 0{,}003\ \mu\text{m} \tag{44}$$

Then, a good estimation for the uncertainty component associated with noise instrument would be:

$$u_{\text{noise}} = \bar{R}_a = 0{,}09\ \mu\text{m} \tag{45}$$

4. Discussion

Table 6 summarize the results obtained during the confocal microscope calibration (section 2)

Table 6. Results of calibration. [1] Non-linearity in Z-axis is included in $s_r(z)$

Parameter	Value	Units	Standard Uncertainty
c_{xy}	0,008 83	-	0,000 50
a	- 0,000 040	-	0,000 036
θ	- 0,000 798	-	0,000 074
c_z	0,010 1	-	0,001 4
$r(c_{xy}, c_z)$	0,72	-	-
u_{FLT}	0,54	µm	-
$u_{\text{NL},xy}$	0,70	µm	-
$s_r(x) = s_r(y)$	0,40	µm	-
$s_r(z)$	0,80 [1]	µm	-
$\bar{b}$	+0,11	µm	0,05
δb	0	µm	0,06
$s(R)$	0,07	µm	
u_{noise}	0,09	µm	

Please note that these results are only valid for measurements made with the same objective (×10). If other objectives are going to be used, a whole re-calibration is needed with each new objective.

Parameters c_{xy} and c_z are those whose effects and their uncertainties the highest. If their effects are not corrected, their contribution to the relative expanded uncertainty would be around 1%.

Fortunatelly, software of confocal microscope permits to introduce their value in order to compensate their effects. If this compensation is done, their contribution to the relative expanded uncertainty is reduced to 0,3%.

The effect of parameter a (difference between pixel lengths along X and Y axes) is negligible. Its absolute value is lower than its expanded uncertainty $U(a) = k \cdot u(a)$ (for $k = 2$), therefore the null hypothesis $a = 0$ cannot be rejected. Its contribution to the relative expanded uncertainty is very low (around 0,01%).

The effect of parameter θ (squareness defect between X and Y axes) seems to be significant (its absolute value is clearly higher than its expanded uncertainty) but its contribution to the relative expanded uncertainty (around 0,1%) is clearly negligible in comparison with c_{xy} and c_z.

Contributions of XY-plane flatness defect (u_{FLT}) and the non-linearity in X and Y axes are clearly lower than the voxels dimensions ($w_{xy} = 1{,}65\ \mu\text{m}$ and $w_z = 2\ \mu\text{m}$). Therefore, the instrument adjustment performed by the manufactured seems to have been good.

Repeatabilities in the XY-plane and in the Z-axis, in comparison with voxels dimensions, are clearly low. Again, this can be used to conclude that the instrument is working well.

Peer-reviewed version available at Materials 2019, 12, 4137; doi:10.3390/ma12244137

In roughness measurements (only apply when using R_a parameter), repeatability $s(R)$, average bias $\overline{b}$, bias variability $u(\delta b)$ and instrument noise u_{noise} are very small in comparison with voxel height $w_z = 2$ µm.

4.1. Expanded Uncertainty Estimation for Length Measurements in the XY-Plane

As it was pointed out, the instrument software usually permits to introduce parameters c_{xy} and c_z in order to apply the corresponding corrections. On the contrary, parameters a and θ cannot be introduced. Therefore, the effect of uncorrected, non-null parameters a and θ would be taken into account as a systematic effect which equivalent standard uncertainty would be respectively $|a|/\sqrt{3}$ and $|\theta|/\sqrt{3}$.

For length measurement performed in plane XY the following expression could be a good estimate of its expanded uncertainty (for a coverage factor $k = 2$), where pixel width component has been estimated as $w_{xy}/\sqrt{12}$ (uniformly distributed between $\pm w_{xy}/2$) :

$$U(L_{xy}) = k \cdot \sqrt{L_{xy}^2 \cdot \left[u^2(c_{xy}) + \frac{a^2}{3} + u^2(a) + \frac{\theta^2}{3} + u^2(\theta)\right] + u_{\text{NL},xy}^2 + s_r^2(x) + \frac{w_{xy}^2}{12}} \leq \leq 1{,}9\ \text{µm} + \frac{L}{1600} \quad (46)$$

4.2. Expanded Uncertainty Estimation for Height Measurements Along the Z-Axis

For height measurement ($0 \leq h \leq 100$ µm, the Z-range approximately covered by the sphere cap measured) the following expression gives us a reasonable estimation of its expanded uncertainty $U(h)$ for a coverage factor $= 2$:

$$U(h) = k \cdot \sqrt{h^2 \cdot u^2(c_z) + u_{\text{FLT}}^2 + s_r^2(z) + \frac{w_z^2}{12}} \leq 2{,}2\ \text{µm} + \frac{h}{120} \quad (47)$$

4.3. Expanded Uncertainty for Roughness Measurements

Following recommendations of documents DKD-R 4-2 [48, 49, 50], a model for a corrected R_a roughness measurement performed after instrument calibration would be:

$$R_a = \bar{R} \cdot (1 + c_z) - (\bar{b} + \delta b) + \delta R_{\text{noise}} \quad (48)$$

Where now, $\bar{R}$ is the average of m repeated measurements made over the specimen being measured and δR_{noise} a random variable of null mean and distributed normally with standard deviation u_{noise}. The standard uncertainty of R_a would be:

$$u(R_a) = \sqrt{\frac{s^2(R)}{m} + \bar{R}^2 \cdot u^2(c_z) + u^2(\bar{b}) + u^2(\delta b) + u_{\text{noise}}^2} \quad (49)$$

The expanded uncertainty $U(R_a)$, using a coverage factor k would be:

$$U(R_a) = k \cdot \sqrt{\frac{s^2(R)}{m} + \bar{R}^2 \cdot u^2(c_z) + u^2(\bar{b}) + u^2(\delta b) + u_{\text{noise}}^2} \quad (50)$$

Considering a coverage factor $k = 2$ and assuming that measurement will be repeated $m = 3$ times, the expanded uncertainty would be:

$$U(R_a) < 0{,}25\ \text{µm} \quad (51)$$

This value is very good for an instrument with a voxel height of $w_z = 2$ µm.

5. Conclusions

A whole calibration procedure to give adequate traceability to confocal microscope used in quality control in AM has been presented. This procedure provides adequate traceability to length and roughness measurements performed with confocal microscopes. The calibration procedure is as simple as possible, as it is designed to be implemented in industrial environment. Reference material standards have been chosen to be easy to find and easy to calibrate again in industrial environments. The calibration procedure covers all the key points of operation of a confocal micrososcope. It permits to estimate:

- Amplification coefficients $\alpha_x = 1 + c_{xy} + a$, $\alpha_y = 1 + c_{xy} - a$ and $\alpha_z = 1 + c_z$
- Non-linearity errors.
- Squareness error θ between X and Y axis.
- Relative difference $2a$ in pixel dimensions along X and Y axis.
- Repeatabilities when measuring lengths or heights.
- Flatness defect in XY-plane.
- Bias deviation b when measuring roughness.
- Instrument noise when measuring roughness.
- Repeatability when measuring roughness.

Some of these parameters (amplification coefficients, flatness defect in XY-plane) can be introduced in the instrument software to compensate their effects. Others cannot be compensated (θ, a) but, if high values are detected the user can ask the instrument manufacturer to adjust and/or repair the instrument to reduce their effects.

Uncertainty estimations have been carried out for all parameters following the mainstream GUM method. In addition, for measurements of lengths and roughness, expression for expanded uncertainties of measurement carried out by the instrument have been provided. There are other types of measurements, like angular measurements, that have not been addressed in the paper due to limitations in the extent of the text. Notwithstanding, all the information needed to propagate uncertainties to angle measurements is provided in the paper.

Author Contributions: Conceptualization, Alberto Mínguez Martínez and Jesús de Vicente y Oliva; Investigation, Alberto Mínguez Martínez; Methodology, Alberto Mínguez Martínez and Jesús de Vicente y Oliva; Software, Alberto Mínguez Martínez and Jesús de Vicente y Oliva; Supervision, Jesús de Vicente y Oliva; Validation, Jesús de Vicente y Oliva; Writing – original draft, Alberto Mínguez Martínez; Writing – review & editing, Jesús de Vicente y Oliva.

Funding: This research received no external funding

Conflicts of interest: The authors declare no conflict of interest.

References

1. Kruth, J.P. Material Incress Manufacturing by Rapid Prototyping Techniques. *CIRP Ann* **1991**, *40*, pp. 603-614. DOI 10.1016/S0007-8506(07)61136-6
2. Levy, G.N.; Schindel, R.; Kruth, J.P. Rapid manufacturing and rapid tooling with layer manufacturing (LM) technologies, state of the art and future perspectives. *CIRP Ann* **2003**, *52*, pp. 589-609. DOI 10.1016/S0007-8506(07)60206-6
3. Zhai, Y.; Lados, D.A.; Lagoy, J.L. Additive Manufacturing: Making Imagination the Major Limitation. *JOM* **2014**, *66*, pp. 808-816. DOI 10.1007/s11837-014-0886-2
4. Huang, Y.; Leu, M.C.; Mazumder, J.; Donmez, A. Additive Manufacturing: Current State, Future Potential, Gaps and Needs, and Recommendations *J Manuf Sci Eng* **2015**, *137*, pp. 014001 1-10. DOI 10.1115/1.4028725
5. Schmidt, M.; Merklein, M.; Bourell, D.; Dimitrov, D.; Hausotte, T.; Wegener, K.; Overmeyer, L.; Vollertsen, F.; Levy, G.N. Laser based additive manufacturing in industry and academia. *CIRP Ann Manuf Technol* **2017**, *66*, pp. 561-583. DOI 10.1016/j.cirp.2017.05.011
6. Chen, L.; He, Y.; Yang, Y.; Niu, S.; Ren, H. The research status and development trend of additive manufacturing technology. *Int J Adv Manuf Technol*, **2017**, *89*, pp. 3651-3660. DOI 10.1007/s00170-016-9335-4

Peer-reviewed version available at *Materials* **2019**, *12*, 4137; doi:10.3390/ma12244137

7. Gibson, I. The changing face of additive manufacturing. *J Manuf Technol Mana*, **2017**, *28*, pp. 10-17. DOI 10.1108/JMTM-12-2016-0182
8. Foxa, J.C.; Moylana, S.P.; Lanea, B.M. Effect of process parameters on the surface roughness of overhanging structures in laser powder bed fusion additive manufacturing. *Procedia CIRP*, **2016**, *45*, pp. 131-134. DOI 10.1016/j.procir.2016.02.347
9. Leach, R.K. Metrology for Additive Manufacturing. *Meas Control – UK*, **2016**, *49*, pp. 132-135. DOI 10.1177/0020294016644479
10. Islam, M.; Boswell, B.; Pramanik, A. Dimensional Accuracy Achievable by Three-Dimensional Printing. In *IAENG Transactions on Engineering Sciences*; Ao, S.I.; Chan, A.H.S.; Katagiri, H.; Xu, L.; Publisher: Taylor & Francis Group, 2014. DOI 10.1201/b16763-29
11. European Committee for Standardization (CEN), *ISO 17296-2:2015 Additive manufacturing. General principles - Part 2: Overview of process categories and feedstock;* CEN: Bruxelles, Belgium, 2015.
12. Turner, B.N.; Gold, S.A. A review of melt extrusion additive manufacturing processes: II. Materials, dimensional accuracy, and surface roughness. *Rapid Prototyp J* **2015**, *3 (21)*, pp. 250-261. DOI 10.1108/RPJ-02-2013-0017
13. Joint Committee for Guides in Metrology (JCGM) *International Vocabulary of Metrology (VIM) - Basic and general concepts and associated terms*, 3rd ed.; JCGM: France 2012.
14. European Committee for Standardization (CEN), *ISO 3274:1996 Geometrical Product Specifications (GPS) Surface texture: Profile method. Nominal characteristics of contact (stylus) instruments;* CEN: Bruxelles, Belgium, 1996.
15. Leach, R.K. Towards a complete framework for calibration of optical surface and coordinate measuring instruments. SPIE Optical Metrology Plenary Session, ICM, Munich, Germany, 26 June 2019.
16. Giusca, C.; Leach, R.K. *Measurement Good Practice Guide (No. 128): Calibration of the metrological characteristics of imaging confocal microscopes (ICMs)*, National Physical Laboratory (NPL), Teddington, Middlesex, United Kingdom, 2012.
17. Minsky, M. Memoir on Inventing the Confocal Scanning Microscope, *Scanning* **1988**, *10(4)*. DOI 10.1002/sca.4950100403
18. Claxton, N.S.; Fellers, T.J.; Davidson, M.W. Laser scanning confocal microscopy. In *Encyclopedia of Medical Devices and Instrumentation*, 2nd ed.; Webster, J.G.; John Wiley & Sons, Inc., Hoboken, New Jersey, USA 2006; pp. 1-37 DOI 10.1002/0471732877.emd291.
19. Watson, T. Fact and Artefact in Confocal Microscopy. *Adv Dent Res* **1997**, *11(4)*, pp. 128-138. DOI 10.1177/08959374970110040901
20. Cheng, C.; Wang, J.; Leach, R.K.; Lu, W.; Liu, X.; Jiang, X. Corrected parabolic fitting for height extraction in confocal microscopy. *Opt Express* **2019**, *27(3)*, pp. 3682-3697. DOI: 10.1364/OE.27.003682
21. Webb, R.H. Confocal optical microscopy. *Rep Prog Phys* **1996**, 59(3), pp. 427-471. DOI 10.1088/0034-4885/59/3/003
22. Webb, R.H. Theoretical Basis of Confocal Microscopy. *Meth. Enzymol*. **1999** *307*, pp. 3-20 DOI 10.1016/s0076-6879(99)07003-2
23. Salerni, G. Uso de la microscopía confocal de reflectancia en dermatología. Dermatol. Argent., 2011, 17(3), pp. 230-235.
24. Confocal Microscopy, Molecular Expressions. Available online: https://micro.magnet.fsu.edu/primer/techniques/confocal/index.html. (Accessed on 26 10 2019).
25. Leach, R.K.; Bourell, D.; Carmignato, S.; Donmez, A.; Senin, N.; Dewulf, W. Geometrical metrology for metal additive manufacturing. *CIRP Ann Manuf Technol* **2019**, *68(2)*, pp. 677-700. DOI 10.1016/j.cirp.2019.05.004
26. Tata, B.V.R.; Raj, B. Confocal laser scanning microscopy: Applications in material science and technology. *Bull. Mater. Sci* **1998**, *21(4)*, pp. 263-278. DOI 10.1007/BF02744951
27. Introduction to Confocal Microscopy. Available online: https://www.olympus-lifescience.com/en/microscope-resource/primer/techniques/confocal/confocalintro/. (Accessed on 26 10 2019).
28. Cohen-Or, D.; Kaufmann, A. Fundamentals of Surface Voxelization. *CVGIP: Graphical Models and Image Processing* **1995**, 57(6), pp. 453-461. DOI 10.1006/gmip.1995.1039
29. Leach, R.K.; Giusca, C.; Haitjema, H.; Evans, C.; Jiang, X. Calibration and verification of areal surface texture measuring instruments. *CIRP Ann Manuf Technol* **2015**, *64(2)*, pp. 797-813. DOI 10.1016/j.cirp.2015.05.010

30. Caja, J.; Sanz, A.; Maresca, P.; Fernández, T.; Wang, C. Some Considerations about the Use of Contact and Confocal Microscopy Methods in Surface Texture Measurement. *Materials* **2018**, 11(8), 1484. DOI 10.3390/ma11081484
31. Wang, C.; Gómez, E.; Yu, Y. Characterization and correction of the geometric errors in using confocal microscope for extended topography measurement. Part I: Models, Algorithms Development and Validation. *Electronics* **2019**, *8(733)*, pp. 1-21. DOI 10.3390/electronics8070733
32. Wang, C.; Gómez, E.; Yu, Y. Characterization and Correction of the Geometric Errors Using a Confocal Microscope for Extended Topography Measurement, Part II: Experimental Study and Uncertainty Evaluation. *Electronics* **2019**, *8(733)*, pp. 1-21. DOI 10.3390/electronics8111217
33. Joint Committee for Guides in Metrology, Working Group 1 (JCGM/WG 1). *JCGM 100:2008 Evaluation of measurement data — Guide to the expression of uncertainty in measurement (GUM)*, 1st ed.; JCGM: France, 2008.
34. European Accreditation (EA). *EA-4/02 - Evaluation of the Uncertainty of Measurement in Calibration*; EA, 2013.
35. European Committee for Standardization (CEN), *ISO/IEC 17025:2017 General requirements for the competence of testing and calibration*, CEN: Bruxelles, Belgium, 2017.
36. SENSOFAR-TECH LTD., *Application Note: Flatness error on imaging confocal microscopes*. Sensofar: Tarrasa, Spain.
37. Centro Español de Metrología (CEM). *Procedimiento DI-035 para la Calibración de Patrones de Planitud de Vidrio.* CEM: Madrid, Spain, 2004.
38. De Vicente, J.; Molpeceres, C.; Guarneros, O.; García-Ballesteros, J. Calibración de Microscopios Confocales. XVII National Congress of Mechanical Engineering. Gijón, Spain, 2008.
39. Guarneros, O.; De Vicente, J.; Maya, M.; Ocaña, J.L.; Molpeceres, C.; García-Ballesteros, J.; Rodríguez, S.; Duran, H. Uncertainty Estimation for Performance Evaluation of a Confocal Microscope as Metrology Equipment. *MAPAN – J Metrol Soc I* **2014**, *29(1)*, pp. 29-42. DOI 10.1007/s12647-013-0060-2
40. De Vicente, J.; Sánchez-Pérez, A.M.; Maresca, P.; Caja, J.; Gómez, E. A model to transform a commercial flatbed scanner into a two-coordinates measuring machine. *Measurement* **2015**, *73*, pp. 304-312. DOI 10.1016/j.measurement.2015.05.029
41. European Committee for Standardization (CEN), *ISO 25178-70 Geometrical product specification (GPS) Surface texture: Areal - Part 70: Material measures*, CEN: Bruxelles, Belgium, 2014.
42. Centro Español de Metrología (CEM). *Procedimiento DI-004 para la Calibración de Medidoras de una Coordenada Vertical.* CEM: Madrid, Spain, 2013.
43. Wang, C.; Caja, J.; Gómez, E.; Maresca, P.; Procedure for Calibrating the Z-axis of a Confocal Microscope: Application for the Evaluation of Structured Surfaces, *Sensors* **2019**, *19(3)*, pp.527-543. DOI 10.3390/s19030527
44. European Committee for Standardization (CEN), *ISO 5436-1:2000 Geometrical Product Specipications (GPS) Surface texture: Profile method. Measurement standards - Part 1: Material measures*, CEN: Bruxelles, Belgium, 2000.
45. Calibration standards, HALLE Präzisions-Kalibriernormale GmbH. Available online: http://halle-normale.de/framesets/englisch/products/products.html. (Accessed on 29 10 2019).
46. Balcon, M.; Carmignato, S.; Savio, E. Performance verification of a confocal microscope for 3D metrology tasks. *Quality - Access to Success* **2012**, *13(5)*, pp. 63-66.
47. De Vicente, J.; Raya, F. Simplified statistical method for uncertainty estimation in coordinate metrology. In Simplified statistical method for uncertainty estimation in coordinate metrology, Bordeaux, France, 1999.
48. Deutscher Kalibrierdienst (DKD), *Guideline DKD 4-2 Calibration of measuring instruments and standards for roughness measuring technique (Sheet 1: Calibration of standards for roughness measuring technique)*, DKD: Braunschweig, Germany, 2011.
49. Deutscher Kalibrierdienst (DKD), *Guideline DKD-R 4-2 Calibration of Devices and Standards for Roughness Metrology (Sheet 2: Calibration of the vertical measuring system of stylus instrument)*, DKD: Braunschweig, Germany, 2011.
50. Deutscher Kalibrierdienst (DKD), *Guideline DKD-R 4-2 Calibration of Devices and Standards for Roughness Metrology (Sheet 3: Calibration of standards with periodic profiles in horizontal direction by means of stylus instrument)*, DKD: Braunschweig, Germany, 2011.
51. European Committee for Standardization (CEN), *ISO 4287:1999 Geometrical Product Specifications (GPS) Surface texture: Profile method. Terms, definitions and surface texture parameters*, CEN: Bruxelles, Belgium, 1999.

Peer-reviewed version available at *Materials* **2019**, *12*, 4137; doi:10.3390/ma12244137

52. European Committee for Standardization (CEN), *ISO 4288:1996 Geometrical product specifications (GPS) Surface Texture: Profile method. Rules and procedures for the assessment of surface texture*, CEN: Bruxelles, Belgium, 1996.
53. Leach, R.K.; Haitjema, H.; Bandwidth characteristics and comparisons of surface texture measuring instruments, *Meas. Sci. Technol.* **2010**, *21(7)* DOI 10.1088/0957-0233/21/7/079801.
54. European Committee for Standardization (CEN), *ISO 25178-6:2010 Geometrical product specification (GPS) Surface texture: Areal - Part 6: Classification methods for measuring surface texture*, CEN: Bruxelles, Belgium, 2010.